

How To Enhance the Efficiency of Breslow Intermediates for SET Catalysis

Florian F. Mulks, Mohand Melaimi, Xiaoyu Yan,* Mu-Hyun Baik,* and Guy Bertrand*



Cite This: *J. Org. Chem.* 2023, 88, 2535–2542



Read Online

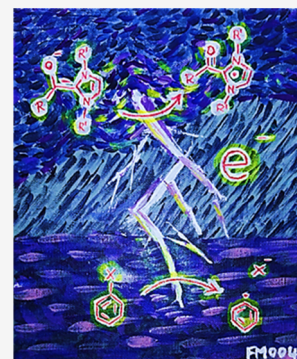
ACCESS |

Metrics & More

Article Recommendations

Supporting Information

ABSTRACT: Oxidative carbene organocatalysis, which proceeds via single electron transfer (SET) pathways, has been limited by the moderately reducing properties of deprotonated Breslow intermediates BI⁻s derived from thiazol-2-ylidene 1 and 1,2,4-triazolylidene 2. Using computational methods, we assess the redox potentials of BI⁻s based on ten different types of known stable carbenes and report our findings concerning the key parameters influencing the steps of the catalytic cycle. From the calculated values of the first oxidation potential of BI⁻s derived from carbenes 1 to 10, it appears that, apart from the diamidocarbene 7, all the others are more reducing than thiazol-2-ylidene 1 and the 1,2,4-triazolylidene 2. We observed that while the reducing power of BI⁻s significantly decreases with increasing solvent polarity, the redox potential of the oxidant can increase at a greater rate, thus facilitating the reaction. The cation, associated with the base, also plays an important role when a nonpolar solvent is used; large and weakly coordinating cations such as Cs⁺ are beneficial. The radical–radical coupling step is probably the most challenging step due to both electronic and steric constraints. Based on our results, we predict that mesoionic carbene 3 and abnormal NHC 4 are the most promising candidates for oxidative carbene organocatalysis.



INTRODUCTION

While stable singlet carbenes have found numerous applications when associated with metals,^{1,2} they also display a rich chemical reactivity on their own merits. Thiazol-2-ylidenes 1³ and 1,2,4-triazolylidenes 2⁴ have been long known to induce umpolung reactivity of carbonyl compounds, giving rise to the formation of nucleophilic Breslow intermediates (BIs).^{5,6} The latter allow for a variety of chemical transformations, which proceed in a well understood ionic mode, via electron-pair-transfer mechanisms. Several decades ago, it was shown that BIs are also involved in single-electron transfer (SET)-based catalysis during the oxidative decarboxylation of pyruvate to form acetyl-CoA.⁷ However, it is only in 2008 that Studer and co-workers⁸ developed a TEMPO-mediated biomimetic oxidation of aldehydes to TEMPO-esters. Since that time, other oxidants, such as nitroarenes, nitroalkenes, CX₄, C₂Cl₆, sulfonic carbamate, redox-active esters, the Togni's reagent, polyfluoroalkyl halides, Katritzky pyridinium salts, oxime ester, and recently aryl iodides (*vide infra*), were also employed to achieve oxidative reactions with aldehydes.⁹

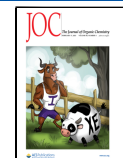
It was initially postulated that the catalytic cycle proceeded through a SET from the BIs leading to the radical cations BI^{•+} which was regarded as the key intermediates. However, mechanistic and electrochemical investigations of standard enols,¹⁰ as well as recent studies, showed that the active paramagnetic species is rather the corresponding neutral radical BI[•].¹¹ Moreover, we showed that the SET does not occur from the BI, but from their deprotonated form, BI⁻.¹¹ Consequently, the catalytic cycle of the oxidative reactions of aldehydes involves six steps, which are described in Figure 1.

So far, with the exception of our work¹² employing mesoionic carbene (MICs) 3,¹³ thiazol-2-ylidenes 1³ and 1,2,4-triazolylidenes 2⁴ have been the only carbenes efficiently used in the catalytic oxidative reactions of aldehydes. Due to the moderately reducing properties of BI⁻s derived from 1 and 2, the reported SET catalyzed reactions require a relatively strong oxidant (*vide supra*), which dramatically limits their synthetic applications. Motivated by the availability of a library of stable singlet carbenes with varying electronic and steric properties, we wondered if we could predict the best candidates to promote these reactions. Obviously, one of the key factors is the reducing power of the BI⁻. Since electrochemical studies are difficult to implement for highly reactive intermediates such as Breslow enolates, we used computational methods to assess the redox potentials of BI⁻s based on a variety of known stable carbenes. We also report our findings concerning each step of the catalytic cycle, including the possible pitfalls.

DFT calculations¹⁴ (in Jaguar 9.1)¹⁵ at the PBE/6-31G**//cc-pVTZ¹⁶ level of theory with the Poisson–Boltzmann solvation model were used for carbenes 1–10 (Figure 2) and their related catalytic intermediates. All molecules and ions

Received: December 12, 2022

Published: January 31, 2023



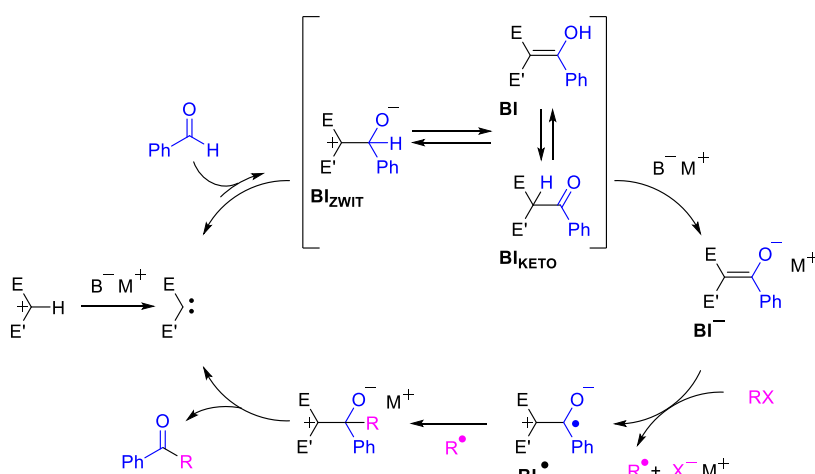


Figure 1. Catalytic cycle for carbene oxidative organocatalytic reactions.

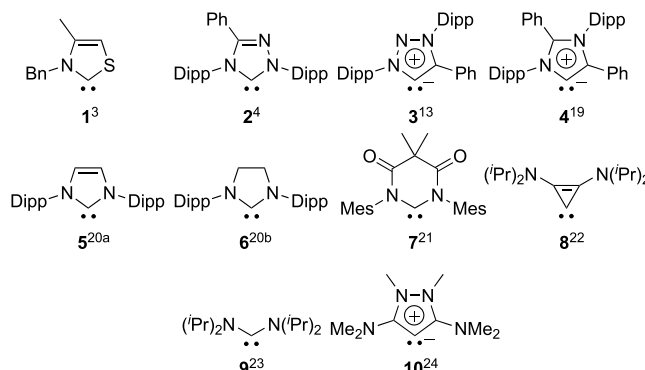


Figure 2. Carbenes considered in this manuscript.

were considered as isolated structures. All redox potentials were computed from solution free energies and referenced to the computed ferrocene/ferrocenium couple.¹⁷ Values are given in acetonitrile unless noted otherwise. To validate our choice of computational methodology, an array of basis set/functionals were evaluated (see Supporting Information (SI)) and the results were compared to known experimental values. Comparison to ten literature-known redox potentials showed an average error of 190 mV with five examples showing an error of 100 mV or less which is in the range of experimental error. Larger errors may indicate the significance of aggregates (contact/solvent-bridged/solvent-separated ion pairs)¹⁸ in some cases under the respective experimental conditions.

RESULTS AND DISCUSSION

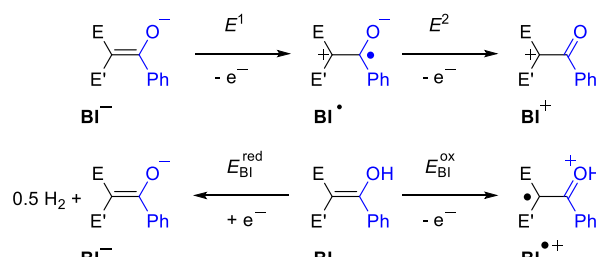
First and Second Oxidation of BI⁻s. We found that the first (E^1) and second (E^2) oxidation potentials of BI⁻s based on carbenes 1–10 and benzaldehyde span over a large range from −1.50 (2) to −2.27 V (5), and −0.31 (7) to −2.43 V (10), respectively (Table 1 and Figure 3).

Because of the rather high computational expense of modeling redox potentials, we also looked into simpler predictive indicators connecting the carbenes' electronic properties and the redox potential of their BI⁻s. The HOMO orbital energies of carbenes 1–10 (and additional examples detailed in the SI) give a rough indication of the redox potential ranking of BI⁻s (Pearson- r : −0.666), but notable outliers exist. For example, the computed redox potentials for the BI⁻s derived from MIC 3 (−2.22 V) and

Table 1. HOMO and LUMO Energies of Carbenes 1–10 and Redox Potentials of the Corresponding BI⁻s and BIs

	HOMO ^a	LUMO ^a	E^1 ^b	E^2 ^b	E_{BI}^{red} ^b	E_{BI}^{ox} ^a
1	−5.05	−1.51	−1.58	−0.72	−1.57	−0.57
2	−5.22	−2.12	−1.50	−0.93	−1.65	−0.61
3	−4.65	−2.14	−2.22	−1.12	−1.94	−0.95
4	−4.29	−2.18	−2.16	−1.59	−2.00	−1.40
5	−4.94	−1.23	−2.27	−1.10	−2.10	−0.88
6	−4.78	−1.12	−1.94	−1.05	−1.97	−0.57
7	−4.99	−2.81	−1.05	−0.31	−1.65	+0.37
8	−4.20	−0.15	−2.26	−1.43	−2.47	−1.06
9	−3.63	+0.15	−1.89	−1.14	−2.16	−0.58
10	−3.59	−0.87	−2.25 ^c	−2.43 ^c	−2.34	−1.91

^aIn eV. ^bIn V. ^cSee SI for more details.

Figure 3. First and second oxidation of BI⁻ (top); reduction and oxidation of BI (bottom).

imidazol-2-ylidene 5 (−2.27 V) are predicted to be comparable, while their HOMO levels are significantly different (−4.65 and −4.94 eV, respectively). Just as for organometallic complexes, the π-accepting ability of carbenes plays a significant role. Thus, a better predictor can easily be obtained using $\frac{1}{2}(e_3^{HOMO} + e_3^{LUMO})$ which is closely related to Mulliken's electronegativity (Pearson- r : −0.74, R^2 : 0.55, Figure 4).²⁵ Indeed, 3-BI⁻ exhibits a lower LUMO than 5-BI⁻ (LUMO: −2.14 and −1.23 eV, respectively) which readily explains that despite its higher HOMO, the reduction power of its BI⁻ is comparable to that of 5.

From these data, it clearly appears that MICs 3¹³ and aNHGs 4¹⁹, which lead to highly reducing BI⁻s, are more promising candidates than thiazol-2-ylidenes 1³ and the 1,2,4-triazolylidenes⁴ that have widely been used for SET catalysis.

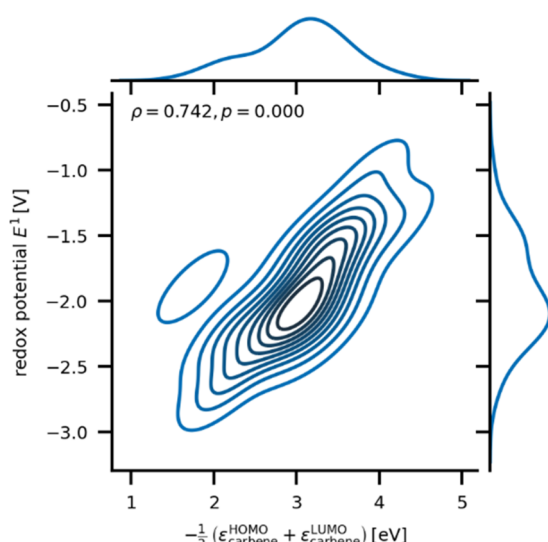


Figure 4. Distribution plot showing the correlation between E^1 and $\frac{1}{2}(\epsilon_3^{HOMO} + \epsilon_3^{LUMO})$ for all computed carbene/ BI^- pairs, see SI for full list.

Their strongly negative redox potential indicates that they can react with weak oxidants.

Oxidation and Reduction of BI's. Because of the earlier assumption that BI's were the active reducing agent, we also calculated their oxidation and reduction potentials. We found that the oxidation of BI's also covers a large range [+0.37 (7) to -1.91 V (10)] and roughly follows the order observed for BI^- 's. Importantly, they are on average 1.1 V less reducing than the corresponding BI^- 's. The resulting $\text{BI}^{\bullet+}$'s are strongly acidic as shown by the predicted large negative pK_a 's (see SI), which readily explain the involvement of the neutral radicals BI^\bullet instead of the radical cations $\text{BI}^{\bullet+}$ in catalysis.¹¹

A reduction process was also experimentally observed by cyclic voltammetry for a Breslow homoenol derived from 6, in the form of an irreversible peak at -1.90 V. The outcome of this process was unclear.¹⁵ Our calculations show that the reduction of the BI derived from 6, computed at -1.97 V, is coupled with a fast or concerted hydrogen evolution resulting in the formation of the corresponding BI^- (see SI).

Interestingly, with some carbenes (1, 3–5), the BI^- can readily reduce the corresponding BI giving BI^\bullet , half an equivalent of H_2 , and regenerating the BI^- . The overall process is the electrocatalytic reduction of BI's into BI^- 's and H_2 . In these cases, this competing pathway could prevent efficient oxidative catalytic processes.

Influence of the Solvent and Cation on the Reducing Properties of BI^- 's.

After examining the role of the carbene, we turned our attention to the influence of the solvent and cation on the reducing properties of BI^- 's. We modeled solvation with a self-consistent reaction field approach (SCRF) and calculated the solvation with 25 distinct dielectric constants in the range of 1 (vacuum) to 100 (Figure 5). Note that this model does not capture dispersion effects or explicit coordination which implies that apolar solvents may not be captured accurately. We observed that the reductant strength of the BI^- significantly decreases with increasing polarity of the solvent, which is a stabilizing factor for charged molecules. For example, the redox potential of the couples $\text{BI}^-/\text{BI}^\bullet$ derived from 1 and 3 shifts from -2.42 and -2.92 V in *t*BuOMe ($\epsilon = 4.5$) to -1.48 and -2.15 V in water ($\epsilon = 78.4$). Therefore, at first glance, we could assume that oxidative catalysis involving BI^- 's should be favored by nonpolar solvents, but this is not necessarily the case, as evidenced by recent work by Ohmiya and co-workers.²⁶ They reported the arylacetylation of styrene in DMSO/H₂O, with phenyl iodide as an oxidant ($E_{pa} = -2.69$ V in CH₃CN), and thiazol-2-ylidene 1 as a catalyst, the BI^- of which has a reported $E_{1/2} = -1.43$ V in CH₃CN. To rationalize this thermodynamically unfavorable reduction, they cite the previous work by Saveant and co-workers²⁷ and wrote “the small reorganization energy of the enolate form of the Breslow intermediate and the fast mesolytic cleavage of the C(sp²)–I bond makes the pathway kinetically feasible”. Interestingly, our calculations show that although the redox potentials of BI^- 's increase with solvent polarity, the redox potential of PhI (PhI → Ph[•] + I⁻) increases at a higher rate. This is mainly due to the larger ion size of the BI^- compared to I⁻; the latter being better stabilized by polar solvents. Consequently, the reaction becomes thermodynamically favorable, as shown by ΔG which decreases from -0.71 in *t*BuOMe to -3.81 kcal·mol⁻¹ in water for 1 (Figure 5, left). In the case of carbene 3, the ΔG changes from -12.63 in

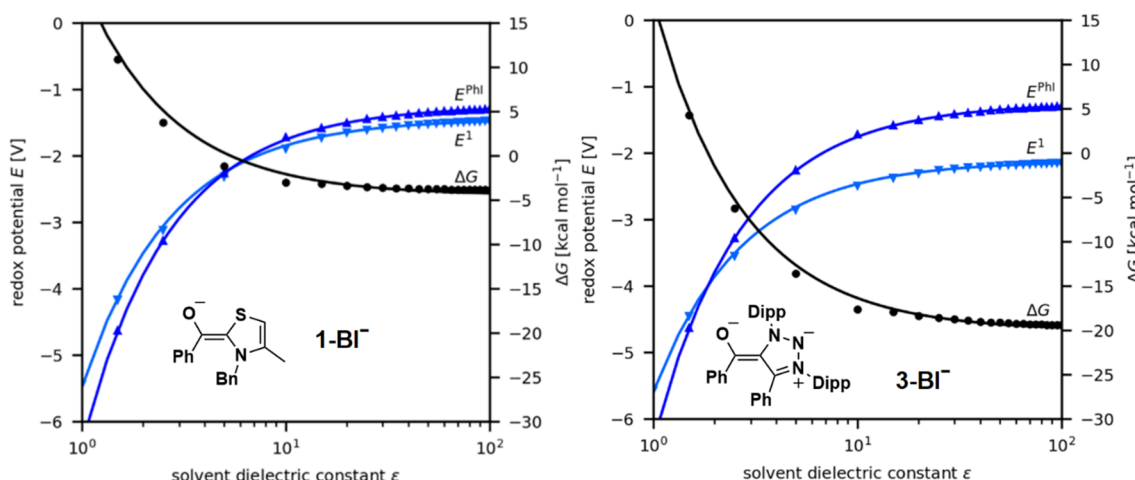


Figure 5. Thermodynamic feasibility of PhI reduction by BI^- responds differently with different carbenes which is illustrated for 1 (left) and 3 (right) with the corresponding redox potentials and the redox reaction's ΔG .

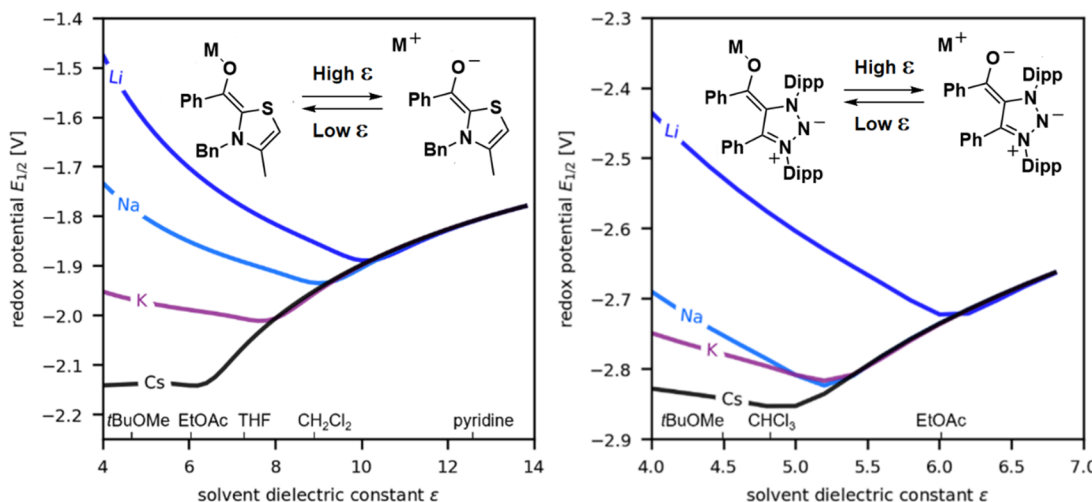


Figure 6. Influence of the cation (Li, N, K, Cs) on the first reduction potential of $\text{BI}^{-}\text{M}^{+}$ salts derived from carbenes 1 (left) and 3 (right) with the solvent polarity.

$t\text{BuOMe}$ to $-19.35 \text{ kcal}\cdot\text{mol}^{-1}$ in water (Figure 5, right). Due to the higher reducing power of MIC 3 compared to thiazol-2-ylidene 1, it is not surprising that the former is able to promote the arylacetylation of styrene in $t\text{BuOMe}$ under milder conditions¹² than those reported for thiazol-2-ylidene 1 in water.²⁶

Regarding the role of the cation, we limited our study to alkali metals (Li, Na, K, and Cs) because of their predominant use as a counterion of the base in oxidative organocatalysis. The salts were modeled, and a Boltzmann two-state distribution was used to predict the respective equilibrium position of the association/dissociation ($\text{BI}^{-}\text{M}^{+} \rightleftharpoons \text{BI}^{-} + \text{M}^{+}$). This model ignores distinct states mediating between isolated and coordinated/contact ion pairs. Particularly the transition area may behave differently due to the formation of solvent-separated or solvent-bridged ion pairs.¹⁸ We used the $1/\epsilon$ dependency of the employed solvation model to inter- and extrapolate from three explicitly computed solvation energies (in CH_3CN $\epsilon = 37.5$, THF $\epsilon = 7.6$, and $t\text{BuOMe}$ $\epsilon = 4.5$). Unsurprisingly, we found that, in polar solvents, the role of the cation is minimal due to the solvent-induced $\text{BI}^{-}/\text{M}^{+}$ separation. In contrast, in nonpolar solvents, the smaller cations significantly increase the redox potential of $\text{BI}^{-}\text{M}^{+}$ (Figure 6). Therefore, large and weakly coordinating cations are beneficial in a nonpolar medium.

Formation of the Deprotonated Breslow Intermediate (BI^{-}). The initial step of the catalytic cycle in carbene oxidative organocatalysis is the deprotonation of the carbene-conjugate acid. Our results, combined with those found in the literature, suggest that even carbonates are basic enough for all carbene precursors, provided that an aldehyde is present to shift the equilibrium.²⁶

The carbene must be nucleophilic enough to react with benzaldehyde in order to obtain the primary form zwitterionic adduct BI_{ZWIR} . We found this step to be endergonic with all carbenes 1–10 (ΔG s ranging from $+3.7$ to $+18.2 \text{ kcal}\cdot\text{mol}^{-1}$), but if we combine this process with the tautomerization into BI or BI_{KETO} , the free enthalpies range from -15.0 (7) to $+11.6 \text{ kcal}\cdot\text{mol}^{-1}$ (10) (Table S9), suggesting that this chemical transformation should be achievable at room temperature with all carbenes 1–10. Note that the BI_{KETO} tautomer is rarely considered, although it has been observed

experimentally. Berkessel and co-workers²⁸ have reported the rearrangement of BI to BI_{KETO} with NHCs of types 5 and 6, and our group has shown that the BI_{KETO} tautomer was the thermodynamic product when cyclic (alkyl)(amino)carbenes²⁹ were reacted with benzaldehyde.³⁰

We calculated the ΔG for the deprotonation of any tautomer of Breslow intermediates using $t\text{BuOK}$ as a base and acetonitrile as the solvent. This process is exergonic for carbenes 1–10 (up to $\Delta G = -24.7 \text{ kcal}\cdot\text{mol}^{-1}$ for thiazol-2-ylidene 1) (Table S6).

Coupling of BI^{\bullet} with Organic Radicals. It is well understood that radical coupling is thermodynamically favorable when both radicals have similar singly occupied molecular orbital (SOMO) energies. We found that the SOMO levels of BI^{\bullet} s generated from carbenes 1–10 lie between -4.06 (7) and -2.65 eV (8), and therefore they are electron-rich radicals (Figure 7). The BI^{\bullet} s derived from the most exploited thiazol-2-ylidene 1 and 1,2,4-triazolylidene 2 are among the least electron-rich of the series (-3.43 and -3.29 eV , respectively). Those derived from carbenes 3–5, 8, and 9 are the most electron-rich examples ($>-2.96 \text{ eV}$). The SOMO energy level of BI^{\bullet} s readily explains the type of coupling partners which have been successfully and unsuccessfully used experimentally thus far. Tertiary alkyl radicals ($t\text{Bu}: -3.66 \text{ eV}$) work very well, but phenyl radicals are far too electron-poor (-5.53 eV) to directly couple with BI^{\bullet} s. However, Ph^{\bullet} can add to carbon–carbon double bonds, such as in styrene, generating a rich benzylic 1,2-diphenylethyl radical (-4.12 eV), which can couple with BI^{\bullet} s. This is the concept of radical relay, which has been successfully used experimentally.^{12,26,9d} Based on the calculated SOMO energy levels, further promising candidates are $i\text{Pr}^{\bullet}$ (-3.99 eV), benzyl^{\bullet} (-4.35 eV), and radicals in α -position of an heteroatom lone pair such as $\text{EtOCH}^{\bullet}\text{CH}_3$ (-3.31 eV). Note also that it is easy to tune the redox potential of some of the BI^{\bullet} s, especially those for which an electron-withdrawing group can be placed in the α -position of the carbene center. For example, in the MIC-derived BI^{\bullet} s series, the replacement of the phenyl group on the carbon atom of 3 by COOMe results in the decrease of the SOMO energy level from -2.85 eV to -3.23 eV .

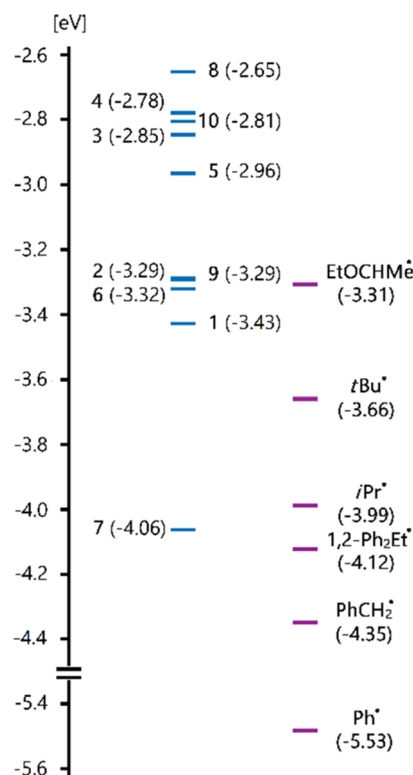


Figure 7. SOMO energy levels of BI^* derived from carbenes 1–10.

The radical–radical coupling step is also probably the most challenging step in carbene oxidative organocatalysis from a steric standpoint. For example, in the MIC-catalyzed arylacylation of styrenes, the replacement of an H by a phenyl group on the carbon next to the carbene center almost entirely suppressed the reaction.¹² Outside of their early discovery and affordable production, a major reason for the success of NHCs like 5 and 6 as ligands in transition metal catalysis is their large steric bulk which improves the reductive elimination step. In contrast, in carbene oxidative organocatalysis, steric bulk hampers the efficiency of the radical–radical coupling step, which can explain the superiority of 1 and 3. To evaluate the steric demands associated with the BI^* 's, we computed their buried volumes (V_{bur}),³¹ a technique usually applied to NHC transition metal complexes.³² The V_{bur} was measured within a sphere of a 3.5 Å radius centered at the carbonyl carbon. Topographic steric maps show the large difference between BI^* 's derived from thiazol-2-ylidene 1 ($1\text{-}\text{BI}^*$) and imidazolylidene 5 ($5\text{-}\text{BI}^*$) in the amount of steric protection (Figure 8). Carbenes known to promote oxidative organocatalytic reactions lead to BI^* with buried volumes below 70%. In the case of 3, substituting the Dipp groups on N atoms with Ph groups and the Ph on the carbon atom with an H atom decreases the V_{bur} from 66% to 52%. In this context, aNHC 4, which is also stable with a hydrogen on the alpha-carbon seems particularly promising, yielding a V_{bur} of 54% with Ph groups in all the other positions.

All carbenes 1–10 are nucleophilic enough to react with benzaldehyde to give the corresponding BIs. However, according to the HOMO energies, the typically used carbenes 1 and 2 are the least nucleophilic of the series, and thus the other carbenes could possibly allow for the use of less electrophilic partners than aryl aldehydes. The deprotonation of the BIs is exergonic in all cases, and thus is not a hurdle.

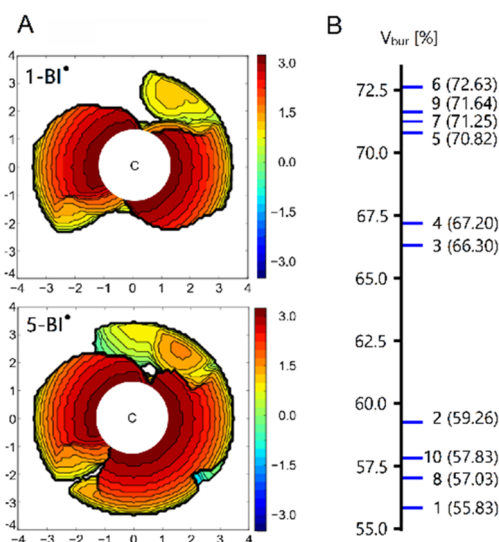


Figure 8. (A) Steric maps of $1\text{-}\text{BI}^*$ and $5\text{-}\text{BI}^*$. (B) Buried volumes of BI^* derived from carbenes 1–10.

From the calculated values of the first oxidation potential of BI^- derived from carbenes 1–10, it clearly appears that, apart from the diamidocarbene 7, all the others are more reducing than thiazol-2-ylidene 1 and the 1,2,4-triazolylidene 2. We observed that the reducing power of BI^- significantly decreases with increasing polarity of the solvent. At first glance, this could imply that oxidative catalysis should be favored by nonpolar solvents, but we found, with PhI as an example, that the redox potential of the oxidant can increase at a higher rate, and thus can facilitate the reaction. The cation, associated with the base used to deprotonate the conjugate acid of the carbenes, also plays an important role when a nonpolar solvent is used; large and weakly coordinating cations such as Cs⁺ are beneficial. The radical–radical coupling step is probably the most challenging step in carbene oxidative organocatalysis due to both electronic and steric constraints. According to the calculated SOMO energy level, all the BI^* 's derived from carbenes 1–10 are electron-rich, which readily explains the type of coupling partners which have been successfully and unsuccessfully used so far experimentally. Among radicals which have not yet been used, we found $^{\prime}\text{Pr}^*$, tolyl*, and radicals in the α -position of a heteroatom lone pair should work. Importantly, the range of the promising radical candidates could be expanded by tuning the redox potential of BI^* 's. This can be readily accomplished for carbenes in which an electron-withdrawing group can be placed in the α -position of the carbene center; MIC 3 and aNHC 4 are excellent candidates. Steric bulk can also hamper the efficiency of the radical–radical coupling step, which can explain the superiority of 1 and 3 over imidazol-2-ylidene 5 and imidazolin-2-ylidene 6, which require bulky substituents on both nitrogen atoms for their stability. In this context, MIC 3 and aNHC 4, which are stable with a hydrogen on the carbon α to the carbene center, appear particularly promising.

EXPERIMENTAL SECTION

Theoretical procedures and details are included in the Supporting Information. This material is available free of charge via the Internet at <http://pubs.acs.org>. The code for some of the data exploration and for making some of the figures can be found at: https://github.com/BaikgrpKAIST/FIGS-BIs_for_SET_catalysis.

■ ASSOCIATED CONTENT

Data Availability Statement

The data underlying this study are available in the published article, in its Supporting Information, and openly available in GitHub at [https://urldefense.com/v3/_https://github.com/Baikgrp/KAIST/FIGS-BIs_for_SET_catalysis_--;!!Mih3wA!C8zqV9pGFD-ZkMn97f81kay3DB_ijcbkEpBCBArelAM8TgSuZePRuDJb0i743Jh9R2-puj_v-ZdDRMgawezxo9kzlOAGJc\\$](https://urldefense.com/v3/_https://github.com/Baikgrp/KAIST/FIGS-BIs_for_SET_catalysis_--;!!Mih3wA!C8zqV9pGFD-ZkMn97f81kay3DB_ijcbkEpBCBArelAM8TgSuZePRuDJb0i743Jh9R2-puj_v-ZdDRMgawezxo9kzlOAGJc$).

● Supporting Information

The Supporting Information is available free of charge at <https://pubs.acs.org/doi/10.1021/acs.joc.2c02978>.

Theoretical procedures and details ([PDF](#))

■ AUTHOR INFORMATION

Corresponding Authors

Guy Bertrand — UCSD-CNRS Joint Research Chemistry Laboratory (UMI 3555), Department of Chemistry and Biochemistry, University of California, San Diego, La Jolla, California 92093-0358, United States;  orcid.org/0000-0003-2623-2363; Email: gbertrand@ucsd.edu

Mu-Hyun Baik — Center for Catalytic Hydrocarbon Functionalizations, Institute for Basic Science (IBS), Daejeon 34141, Republic of Korea; Department of Chemistry, Korea Advanced Institute of Science and Technology (KAIST), Daejeon 34141, Republic of Korea;  orcid.org/0000-0002-8832-8187; Email: mbaik2805@kaist.ac.kr

Xiaoyu Yan — Department of Chemistry, Renmin University of China, Beijing 100872, People's Republic of China;  orcid.org/0000-0003-3973-3669; Email: yanxy@ruc.edu.cn

Authors

Florian F. Mulks — Center for Catalytic Hydrocarbon Functionalizations, Institute for Basic Science (IBS), Daejeon 34141, Republic of Korea; Department of Chemistry, Korea Advanced Institute of Science and Technology (KAIST), Daejeon 34141, Republic of Korea; UCSD-CNRS Joint Research Chemistry Laboratory (UMI 3555), Department of Chemistry and Biochemistry, University of California, San Diego, La Jolla, California 92093-0358, United States; Present Address: Institute of Organic Chemistry (iOC), RWTH Aachen University, Landoltweg 1, 52074 Aachen, Germany;  orcid.org/0000-0003-4140-002X

Mohand Melaimi — UCSD-CNRS Joint Research Chemistry Laboratory (UMI 3555), Department of Chemistry and Biochemistry, University of California, San Diego, La Jolla, California 92093-0358, United States

Complete contact information is available at:
<https://pubs.acs.org/doi/10.1021/acs.joc.2c02978>

Author Contributions

Calculations were performed by F.F.M. All authors conceived and designed the project, analyzed the data and wrote the manuscript.

Notes

The authors declare no competing financial interest.

■ ACKNOWLEDGMENTS

F.F.M. is grateful to the Alexander von Humboldt Foundation for a Feodor Lynen Research Fellowship. The authors thank

Dr. Danilo M. Lustosa for the helpful discussions. Thanks are due to the NSF (CHE-2153475) (G.B.) and the Institute for Basic Science (IBS-R10-A1) in Korea (M.H.B.) for financial support.

■ REFERENCES

- (1) The submitted version of this manuscript was uploaded to the ChemRxiv preprint repository, 10.26434/chemrxiv-2022-ms154.
- (2) For recent reviews, see for examples: (a) Huynh, H. V. Electronic Properties of N-Heterocyclic Carbenes and Their Experimental Determination. *Chem. Rev.* **2018**, *118*, 9457–9492. (b) Gardiner, M. G.; Ho, C. C. Recent advances in bidentate bis(N-heterocyclic carbene) transition metal complexes and their applications in metal-mediated reactions. *Coord. Chem. Rev.* **2018**, *375*, 373–388. (c) Yong, X. F.; Thurston, R.; Ho, C. Y. Electronic Effects on Chiral NHC–Transition-Metal Catalysis. *Synthesis* **2019**, *51*, 2058–2080. (d) Liang, Q.; Song, D. Iron N-heterocyclic carbene complexes in homogeneous catalysis. *Chem. Soc. Rev.* **2020**, *49*, 1209–1032. (e) Zhao, Q.; Meng, G.; Nolan, S. P.; Szostak, M. N-Heterocyclic Carbene Complexes in C–H Activation Reactions. *Chem. Rev.* **2020**, *120*, 1981–2048. (f) Jazzaar, R.; Soleilhavoup, M.; Bertrand, G. Cyclic (Alkyl) and (Aryl)(amino)carbene Coinage Metal Complexes and Their Applications. *Chem. Rev.* **2020**, *120*, 4141–4168. (g) Scattolin, T.; Nolan, S. P. Synthetic Routes to Late Transition Metal–NHC Complexes. *Trends Chem.* **2020**, *2*, 721–736. (h) Morvan, J.; Mauduit, M.; Bertrand, G.; Jazzaar, R. Cyclic (Alkyl)(amino)carbenes (CAACs) in Ruthenium Olefin Metathesis. *ACS Catal.* **2021**, *11*, 1714–1748. (i) Bellotti, P.; Koy, M.; Hopkinson, M. N.; Glorius, F. Recent advances in the chemistry and applications of N-heterocyclic carbenes. *Nat. Rev. Chem.* **2021**, *5*, 711–725.
- (3) Arduengo, A. J., III; Goerlich, J. R.; Marshall, W. J. A Stable Thiazol-2-ylidene and Its Dimer. *Liebigs Ann.* **1997**, *1997*, 365–374.
- (4) Enders, D.; Breuer, K.; Raabe, G.; Runsink, J.; Teles, J. H.; Melder, J. P.; Ebel, K.; Brode, S. Preparation, Structure, and Reactivity of 1,3,4-Triphenyl-4,5-dihydro-1H-1,2,4-triazol-5-ylidene, a New Stable Carbene. *Angew. Chem., Int. Ed.* **1995**, *34*, 1021–1023.
- (5) For reviews, see: (a) Pareek, M.; Reddi, Y.; Sunoj, R. B. Tale of the Breslow intermediate, a central player in N-heterocyclic carbene organocatalysis: then and now. *Chem. Sci.* **2021**, *12*, 7973–7992. (b) Wang, M. H.; Scheidt, K. A. Cooperative Catalysis and Activation with N-Heterocyclic Carbenes. *Angew. Chem., Int. Ed.* **2016**, *55*, 14912–4922. (c) Flanigan, D. L.; Romanov-Michailidis, F.; White, N. A.; Rovis, T. Organocatalytic Reactions Enabled by N-Heterocyclic Carbenes. *Chem. Rev.* **2015**, *115*, 9307–9387. (d) Biju, A. T. N-Heterocyclic Carbenes in Organocatalysis. Wiley-VCH Verlag GmbH & Co KGaA: Weinheim, Germany, 2019. (e) Chen, X.-Y.; Gao, Z.-H.; Ye, S. Bifunctional N-Heterocyclic Carbenes Derived from L-Pyroglutamic Acid and Their Applications in Enantioselective Organocatalysis. *Acc. Chem. Res.* **2020**, *53*, 690–702. (f) Ghosh, A.; Biju, A. T. Revealing the Similarities of α,β -Unsaturated Iminiums and Acylazoliums in Organocatalysis. *Angew. Chem., Int. Ed.* **2021**, *60*, 13712–13724. (g) Ishii, T.; Nagao, K.; Ohmiya, H. Recent advances in N-heterocyclic carbene-based radical catalysis. *Chem. Sci.* **2020**, *11*, 5630–5636. (h) Ohmiya, H. N-Heterocyclic Carbene-Based Catalysis Enabling Cross-Coupling Reactions. *ACS Catal.* **2020**, *10*, 6862–6869. (i) De Risi, C.; Brandolese, A.; Di Carmine, G.; Ragni, D.; Massi, A.; Bortolini, O. Oxidative N-Heterocyclic Carbene Catalysis. *Chem.—Eur. J.* **2023**, *29*, e202202467.
- (6) (a) Breslow, R. On the Mechanism of Thiamine Action. IV. Evidence from Studies on Model Systems. *J. Am. Chem. Soc.* **1958**, *80*, 3719–3726. (b) Berkessel, A.; Elfert, S.; Yatham, V. R.; Neudörfl, J.-M.; Schlörer, N. E.; Teles, J. H. Umpolung by N-Heterocyclic Carbenes: Generation and Reactivity of the Elusive 2,2-Diamino Enols (Breslow Intermediates). *Angew. Chem., Int. Ed.* **2012**, *51*, 12370–12374. (c) Paul, M.; Neudörfl, J. M.; Berkessel, A. Breslow intermediates from a thiazolin-2-ylidene and fluorinated aldehydes: XRD and solution-phase NMR spectroscopic characterization. *Angew.*

- Chem., Int. Ed.* **2019**, *58*, 10596–10600. (d) Berkessel, A.; Yatham, V. R.; Elfert, S.; Neudörfl, J.-M. Characterization of the Key Intermediates of Carbene-Catalyzed Umpolung by NMR Spectroscopy and X-Ray Diffraction: Breslow Intermediates, Homoenolates, and Azolium Enolates. *Angew. Chem., Int. Ed.* **2013**, *52*, 11158–11162. (e) Wessels, A.; Klussmann, M.; Breugst, M.; Schlorer, N. E.; Berkessel, A. Formation of Breslow Intermediates from N-Heterocyclic Carbene and Aldehydes Involves Autocatalysis by the Breslow Intermediate, and a Hemiacetal. *Angew. Chem., Int. Ed.* **2022**, *61*, e202117682. (f) Kusakabe, M.; Nagao, K.; Ohmiya, H. Radical Relay Trichloromethylacylation of Alkenes through N-Heterocyclic Carbene Catalysis. *Org. Lett.* **2021**, *23*, 7242–7247. (g) Ota, K.; Nagao, K.; Ohmiya, H. N-Heterocyclic Carbene-Catalyzed Radical Relay Enabling Synthesis of δ -Ketocarbonyls. *Org. Lett.* **2020**, *22*, 3922–3925. (h) Meng, Q.-Y.; Lezius, L.; Studer, A. Benzylidic C–H Acylation by Cooperative NHC and Photoredox Catalysis. *Nat. Commun.* **2021**, *12*, 2068. (i) Leifert, D.; Studer, A. The Persistent Radical Effect in Organic Synthesis. *Angew. Chem., Int. Ed.* **2020**, *59*, 74–108.
- (7) Ragsdale, S. W. Pyruvate Ferredoxin Oxidoreductase and Its Radical Intermediate. *Chem. Rev.* **2003**, *103*, 2333–2346.
- (8) Guin, J.; De Sarkar, S.; Grimme, S.; Studer, A. Biomimetic Carbene-Catalyzed Oxidations of Aldehydes Using TEMPO. *Angew. Chem., Int. Ed.* **2008**, *47*, 8727–8730.
- (9) (a) White, N. A.; Rovis, T. Enantioselective N-Heterocyclic Carbene-Catalyzed β -Hydroxylation of Enals Using Nitroarenes: An Atom Transfer Reaction That Proceeds via Single Electron Transfer. *J. Am. Chem. Soc.* **2014**, *136*, 14674–14677. (b) Yang, W.; Hu, W.; Dong, X.; Li, X.; Sun, J. N-Heterocyclic Carbene Catalyzed γ -Dihalomethylation of Enals by Single-Electron Transfer. *Angew. Chem., Int. Ed.* **2016**, *55*, 15783–15786. (c) Ishii, T.; Kake-no, Y.; Nagao, K.; Ohmiya, H. N-Heterocyclic Carbene-Catalyzed Decarboxylative Alkylation of Aldehydes. *J. Am. Chem. Soc.* **2019**, *141*, 3854–3858. (d) Ishii, T.; Ota, K.; Nagao, K.; Ohmiya, H. N-Heterocyclic Carbene-Catalyzed Radical Relay Enabling Vicinal Alkylacylation of Alkenes. *J. Am. Chem. Soc.* **2019**, *141*, 14073–14077. (e) Li, J.-L.; Liu, Y.-Q.; Zou, W.-L.; Zeng, R.; Zhang, X.; Liu, Y.; Han, B.; Leng, H.-J.; Li, Q.-Z. Radical Acylfluoroalkylation of Olefins through N-Heterocyclic Carbene Organocatalysis. *Angew. Chem., Int. Ed.* **2020**, *59*, 1863–1870. (f) Kim, I.; Im, H.; Lee, H.; Hong, S. N-Heterocyclic carbene-catalyzed deaminative cross-coupling of aldehydes with Katsirizky pyridinium salts. *Chem. Sci.* **2020**, *11*, 3192–3197. (g) Gao, Y.; Quan, Y.; Li, Z.; Gao, L.; Zhang, Z.; Zou, X.; Yan, R.; Qu, Y.; Guo, K. Organocatalytic Three-Component 1,2-Cyanoalkylacylation of Alkenes via Radical Relay. *Org. Lett.* **2021**, *23*, 183–189. (h) Yang, H.-B.; Wan, D.-H. C–C Bond Acylation of Oxime Ethers via NHC Catalysis. *Org. Lett.* **2021**, *23*, 1049–1053. (i) Jin, S.; Sui, X.; Haug, G. C.; Nguyen, V. D.; Dang, H. T.; Arman, H. D.; Larionov, O. V. N-Heterocyclic Carbene-Photocatalyzed Tricomponent Regioselective 1,2-Diacylation of Alkenes Illuminates the Mechanistic Details of the Electron Donor–Acceptor Complex-Mediated Radical Relay Processes. *ACS Catal.* **2022**, *12*, 285–294.
- (10) (a) Schmittel, M.; Baumann, U. Stability and Cyclization of Enol Radical Cations: A Mechanistic Study of One-Electron Oxidation of β,β -Dimesityl Enols. *Angew. Chem., Int. Ed. Engl.* **1990**, *29*, 541–543. (b) Schmittel, M.; Röck, M. Enol cation radicals in solution. 3. Reaction of enol cation radicals in the presence of nucleophiles. *Chem. Ber.* **1992**, *125*, 1611–1620. (c) Röck, M.; Schmittel, M. Enol cation radicals in solution. 4. An improved Synthesis of 4,6,7-Trimethylbenzofurans by oxidation of β -mesityl substituted enols. *J. Prakt. Chem.* **1994**, *336*, 325–329. (d) Schmittel, M.; Gescheidt, G.; Röck, M. The First Spectroscopic Identification of an Enol Radical Cation in Solution: The Anisyldimesitylethenol Radical Cation. *Angew. Chem., Int. Ed. Engl.* **1994**, *33*, 1961–1963. (e) Schmittel, M.; Lal, M.; Lal, R.; Röck, M.; Langels, A.; Rappoport, Z.; Basheer, A.; Schlirf, J.; Deiseroth, H.-J.; Flörke, U.; Gescheidt, G. A comprehensive picture of the one-electron oxidation chemistry of enols, enolates and α -carbonyl radicals: oxidation potentials and characterization of radical intermediates. *Tetrahedron* **2009**, *65*, 10842–10855.
- (11) (a) Regnier, V.; Romero, E. A.; Molton, F.; Jazza, R.; Bertrand, G.; Martin, D. What are the Radical Intermediates in Oxidative N-Heterocyclic Carbene Organocatalysis? *J. Am. Chem. Soc.* **2019**, *141*, 1109–1117. (b) Delfau, L.; Nichilo, S.; Molton, F.; Brogi, J.; Tomás-Mendivil, E.; Martin, D. Critical Assessment of the Reducing Ability of Breslow-type Derivatives and Implications for Carbene-Catalyzed Radical Reactions. *Angew. Chem., Int. Ed.* **2021**, *60*, 26783–26789.
- (12) Liu, W.; Viana, A.; Zhang, Z.; Huang, S.; Huang, L.; Melaimi, M.; Bertrand, G.; Yan, X. Mesoionic Carbene-Breslow Intermediates as Super Electron Donors: Application to the Metal-Free Arylacylation of Alkenes. *Chem. Catal.* **2021**, *1*, 196–206.
- (13) (a) Guisado-Barrios, G.; Bouffard, J.; Donnadieu, B.; Bertrand, G. Crystalline 1H-1,2,3-Triazol-5-ylidenes: New Stable Mesoionic Carbenes (MICs). *Angew. Chem., Int. Ed.* **2010**, *49*, 4759–4762. (b) Guisado-Barrios, G.; Soleilhavoup, M.; Bertrand, G. 1H-1,2,3-Triazol-5-ylidenes: Readily Available Mesoionic Carbenes. *Acc. Chem. Res.* **2018**, *51*, 3236–3244.
- (14) Parr, R. G.; Weitao, Y. Density-Functional Theory of Atoms and Molecules; Oxford University Press: 1994.
- (15) Bochevarov, A. D.; Harder, E.; Hughes, T. F.; Greenwood, J. R.; Braden, D. A.; Philipp, D. M.; Rinaldo, D.; Halls, M. D.; Zhang, J.; Friesner, R. A. Jaguar: A High-Performance Quantum Chemistry Software Program with Strengths in Life and Materials Sciences. *Int. J. Quantum Chem.* **2013**, *113*, 2110–2142.
- (16) (a) Perdew, J. P.; Burke, K.; Ernzerhof, M. Generalized Gradient Approximation Made Simple. *Phys. Rev. Lett.* **1996**, *77*, 3865–3868. (b) Krishnan, R.; Binkley, J. S.; Seeger, R.; Pople, J. A. Self-consistent Molecular Orbital Methods. XX. A Basis Set for Correlated Wave Functions. *J. Chem. Phys.* **1980**, *72*, 650–654. (c) Dunning, T. H. Gaussian Basis Sets for Use in Correlated Molecular Calculations. I. The Atoms Boron through Neon and Hydrogen. *J. Chem. Phys.* **1989**, *90*, 1007–1023.
- (17) (a) Baik, M.-H.; Friesner, R. A. Computing Redox Potentials in Solution: Density Functional Theory as A Tool for Rational Design of Redox Agents. *J. Phys. Chem. A* **2002**, *106*, 7407–7412. (b) Roy, L. E.; Jakubikova, E.; Guthrie, M. G.; Batista, E. R. Calculation of One-Electron Redox Potentials Revisited. Is It Possible to Calculate Accurate Potentials with Density Functional Methods? *J. Phys. Chem. A* **2009**, *113*, 6745–6750.
- (18) (a) Fuoss, R. M. Ionic Association. III. The Equilibrium between Ion Pairs and Free Ions. *J. Am. Chem. Soc.* **1958**, *80*, 5059–5061. (b) Winstein, S.; Clippinger, E.; Fainberg, A. H.; Heck, R.; Robinson, G. C. Salt Effects and Ion Pairs in Solvolysis and Related Reactions. III. Common Ion Rate Depression and Exchange of Anions during Acetolysis. *J. Am. Chem. Soc.* **1956**, *78*, 328–335. (c) Marcus, R. A.; Sutin, N. Electron transfers in chemistry and biology. *Biochim. Biophys. Acta* **1985**, *811*, 265–322. (d) Fumino, K.; Stange, P.; Fossog, V.; Hempelmann, R.; Ludwig, R. Equilibrium of Contact and Solvent-Separated Ion Pairs in Mixtures of Protic Ionic Liquids and Molecular Solvents Controlled by Polarity. *Angew. Chem., Int. Ed.* **2013**, *52*, 12439–12442.
- (19) (a) Aldeco-Perez, E.; Rosenthal, A. J.; Donnadieu, B.; Parameswaran, P.; Frenking, G.; Bertrand, G. Isolation of a C-5-Deprotoxinated Imidazolium, a Crystalline “Abnormal” N-Heterocyclic Carbene. *Science* **2009**, *326*, 556–559. (b) Sau, S. C.; Hota, P. K.; Mandal, S. K.; Soleilhavoup, M.; Bertrand, G. Stable Abnormal N-Heterocyclic Carbenes and their Applications. *Chem. Soc. Rev.* **2020**, *49*, 1233–1252.
- (20) (a) Arduengo, A. J., III; Harlow, R. L.; Kline, M. A Stable Crystalline Carbene. *J. Am. Chem. Soc.* **1991**, *113*, 361–363. (b) Arduengo, A. J., III; Goerlich, J. R.; Marshall, W. J. A Stable Diaminocarbene. *J. Am. Chem. Soc.* **1995**, *117*, 11027–11028.
- (21) Hudnall, T. W.; Bielawski, C. W. An N,N'-Diamidocarbene: Studies in C–H Insertion, Reversible Carbonylation, and Transition-Metal Coordination Chemistry. *J. Am. Chem. Soc.* **2009**, *131*, 16039–16040.

- (22) Lavallo, V.; Canac, Y.; Donnadieu, B.; Schoeller, W. W.; Bertrand, G. Cyclopropenylidenes: From Interstellar Space to an isolated Derivative in the Laboratory. *Science* **2006**, *312*, 722–724.
- (23) Alder, R. W.; Allen, P. R.; Murray, M.; Orpen, A. G. Bis(diisopropylamino)carbene. *Angew. Chem., Int. Ed. Engl.* **1996**, *35*, 1121–1123.
- (24) Lavallo, V.; Dyker, C. A.; Donnadieu, B.; Bertrand, G. Synthesis and Ligand Properties of Stable Five-Membered Ring Allenes Composed of Second Row Elements. *Angew. Chem., Int. Ed.* **2008**, *47*, 5411–5414.
- (25) (a) Pearson, R. G. Absolute electronegativity and hardness correlated with molecular orbital theory. *Proc. Natl. Acad. Sci. U.S.A.* **1986**, *83*, 8440–8441. (b) Messelberger, J.; Grünwald, A.; Goodner, S. J.; Zeilinger, F.; Pinter, P.; Miehlich, M. E.; Heinemann, F. W.; Hansmann, M. M.; Munz, D. Aromaticity and Sterics Control Whether a Cationic Olefin Radical Is Resistant to Disproportionation. *Chem. Sci.* **2020**, *11*, 4138–4149.
- (26) Matsuki, Y.; Ohnishi, N.; Kakeno, Y.; Takemoto, S.; Ishii, T.; Nagao, K.; Ohmiya, H. Aryl radical-mediated N-heterocyclic carbene catalysis. *Nat. Commun.* **2021**, *12*, 3848.
- (27) Pause, L.; Robert, M.; Savéant, J.-M. Can single-electron transfer break an aromatic carbon–heteroatom bond in one step? A novel example of transition between stepwise and concerted mechanisms in the reduction of aromatic iodides. *J. Am. Chem. Soc.* **1999**, *121*, 7158–7159.
- (28) Paul, M.; Peckelsen, K.; Thomulka, T.; Martens, J.; Berden, G.; Oomens, J.; Neudorfl, J. M.; Breugst, M.; Meijer, A. J. H. M.; Schafer, M.; Berkessel, A. Breslow Intermediates (Amino Enols) and Their Keto Tautomers: First Gas-Phase Characterization by IR Ion Spectroscopy. *Chem.—Eur. J.* **2021**, *27*, 2662–2669.
- (29) For reviews on CAACs, see: (a) Soleilhavoup, M.; Bertrand, G. Cyclic (alkyl)(amino)carbenes (CAACs): Stable carbenes on the rise. *Acc. Chem. Res.* **2015**, *48*, 256–266. (b) Paul, U. S. D.; Radius, U. What Wanzlick did not dare to dream: cyclic (alkyl)(amino)carbenes (caacs) as new key players in transition-metal chemistry. *Eur. J. Inorg. Chem.* **2017**, *2017*, 3362–3375. (c) Melaimi, M.; Jazzaar, R.; Soleilhavoup, M.; Bertrand, G. Cyclic (alkyl)(amino)carbenes (CAACs): Recent developments. *Angew. Chem., Int. Ed.* **2017**, *56*, 10046–10068. (d) Jazzaar, R.; Soleilhavoup, M.; Bertrand, G. Cyclic (alkyl)- and (aryl)-(amino)carbene coinage metal complexes and their applications. *Chem. Rev.* **2020**, *120*, 4141–4168. (e) Kushvaha, S. K.; Mishra, A.; Roesky, H. W.; Mandal, K. C. Recent Advances in the Domain of Cyclic (Alkyl)(Amino) Carbenes *Chem. Asian. J.* **2022**, e202101301.
- (30) Martin, D.; Canac, Y.; Lavallo, V.; Bertrand, G. Comparative Reactivity of Different Types of Stable Cyclic and Acyclic Mono- and Di-Amino Carbenes with Simple Organic Substrates. *J. Am. Chem. Soc.* **2014**, *136*, 5023–5030.
- (31) (a) Luchini, G.; Paton, R. S. DBSTEP: DFT Based Steric Parameters. DOI: [10.5281/zenodo.4702097](https://doi.org/10.5281/zenodo.4702097). (b) Falivene, L.; Cao, Z.; Petta, A.; Serra, L.; Poater, A.; Oliva, R.; Scarano, V.; Cavallo, L. Towards the Online Computer-Aided Design of Catalytic Pockets. *Nat. Chem.* **2019**, *11*, 872–879.
- (32) For use of buried volume on organic compounds, see the following publication and references therein: Sowndarya S V, S.; St. John, P. C.; Paton, R. S. A quantitative metric for organic radical stability and persistence using thermodynamic and kinetic features. *Chem. Sci.* **2021**, *12*, 13158.

□ Recommended by ACS

Construction of Functionalized 2*H*-Pyran-2-ones via N-Heterocyclic Carbene-Catalyzed [3 + 3] Annulation of Alkynyl Esters with Enolizable Ketones

Zheng Liang, Ding Du, et al.

JANUARY 25, 2023

THE JOURNAL OF ORGANIC CHEMISTRY

READ ▶

Triphenylcyclopentadienyl Rhodium Complexes in Catalytic C–H Annulations. Application for Synthesis of Natural Isocoumarins

Vladimir B. Kharitonov, Dmitry A. Loginov, et al.

FEBRUARY 09, 2023

THE JOURNAL OF ORGANIC CHEMISTRY

READ ▶

Fragment Coupling Approach to Diaporthein B

Ian Tingyung Hsu and Seth B. Herzon

FEBRUARY 03, 2023

THE JOURNAL OF ORGANIC CHEMISTRY

READ ▶

Nickel-Catalyzed Sodium Hypophosphite-Participated Direct Hydrophosphonylation of Alkyne toward *H*-Phosphinates

Dang-Wei Qian, Shang-Dong Yang, et al.

FEBRUARY 24, 2023

THE JOURNAL OF ORGANIC CHEMISTRY

READ ▶

Get More Suggestions >